

EFFECTS OF EARTHWORM BURROWING ON ARSENIC
BIOTRANSFORMATION AND MOBILITY: IMPLICATIONS FOR
ROXARSONE-BEARING POULTRY LITTER APPLICATION

By

Aaron K. Covey

Thesis

Submitted to the Faculty of the
Graduate School of Vanderbilt University
In partial fulfillment of the requirements
for the degree of

MASTER OF SCIENCE

in

Earth and Environmental Sciences

December, 2008

Nashville, Tennessee

Approved:

Professor Kaye S. Savage

Professor John C. Ayers

To my wife, Lauren

And

To my parents, William and Norma

ACKNOWLEDGEMENTS

I am grateful to Dr. Kaye Savage for her friendship, encouragement, motivation, and advice throughout this adventure. I would also like to thank my fellow graduate students and professors that have shared in the journey with me, thanks for the support!

Portions of this research were carried out at the Stanford Synchrotron Radiation Lightsource, a national user facility operated by Stanford University on behalf of the U.S. Department of Energy, Office of Basic Energy Sciences. The SSRL Structural Molecular Biology Program is supported by the Department of Energy, Office of Biological and Environmental Research, and by the National Institutes of Health, National Center for Research Resources, Biomedical Technology Program.

PNC/XOR facilities at the Advanced Photon Source, and research at these facilities, are supported by the US Department of Energy - Basic Energy Sciences, a major facilities access grant from NSERC, the University of Washington, Simon Fraser University and the Advanced Photon Source. Use of the Advanced Photon Source is also supported by the U. S. Department of Energy, Office of Science, Office of Basic Energy Sciences, under Contract DE-AC02-06CH11357.

I would like to thank Dr. Max Reams and Sondra Sixberry for their enthusiasm in teaching and guidance in life. You both are truly astounding role models.

I am forever grateful to those closest to me, my family and friends, whose immeasurable love and prayers got me through to the end. Special thanks to my wife, Lauren, for her love, support, and motivation!

Most importantly, I would like to thank my God for all the many blessings.

TABLE OF CONTENTS

	Page
DEDICATION	II
ACKNOWLEDGEMENTS	III
LIST OF TABLES	VI
LIST OF FIGURES	VII
Chapter	
I. INTRODUCTION	1
Arsenic in Poultry Litter	2
Arsenic Toxicity	3
Earthworms	4
Study Scope	7
II. MATERIALS AND METHODS	8
Artificial Soil	8
Mesocosm Construction	8
Bioturbation Columns	9
Arsenic Mobility and Speciation Columns	11
Inductively Coupled Plasma Mass Spectrometry (ICP-MS) Analysis	12
Synchrotron X-ray Microprobe and X-ray Absorption Spectra	13
III. EXPERIMENT 1: BIOTURBATION MESOCOSMS	15
Model Introduction	15
Methods	18
Development of Model	18
Results	21
Effects of Model Fit Values	21
Without Worm or Added Water	23
With Worm, Without Added Water	23
With Added Water, Without Worm	24
With Worm and Added Water	25

IV. EXPERIMENT 2: ARSENIC MOBILITY AND SPECIATION MESOCOSMS	27
Synchrotron X-ray Absorption Spectroscopy (XAS).....	27
Microprobe Imaging Results	28
X-ray Absorption Near Edge Structure ANES Results	30
Arsenic Redistribution.....	32
V. DISCUSSION.....	35
Soil Mixing.....	35
Bioturbation Rates	35
Redistribution Potential	36
Effects of Bioturbation	36
Hydrologic Effects of Burrows	37
Potential Outcomes of Bioturbation	38
Biotransformation and Degradation	40
Methylation along the Drilosphere.....	41
Arsenic Speciation within Earthworm	42
VI. CONCLUSIONS AND IMPLICATIONS.....	43
Appendix	
A. MATLAB MODEL CODE.....	45
REFERENCES	47

LIST OF TABLES

Table	Page
1. Model Experiment Mesocosms.....	11
2. Model values used to fit experimental column data.	25
3. White-line Peak Positions of Standards and Experimental Samples	33

LIST OF FIGURES

Figure	Page
1. Chemical structure of roxarsone.....	1
2. Thermodynamic stability fields for As compounds.	3
3. Experimental setup for mesocosm studies.....	9
4. Mesocosm designs for column experiments.....	10
5. Representation of X-ray equipment setup used at SSRL.	13
6. Schematic of random walk probability position.....	18
7. Effects of changing model fit values.	22
8. Control mesocosm model results.....	23
9. Earthworm bioturbation mesocosm model results.	24
10. Aqueous control mesocosm model results.	26
11. The combination of earthworm burrows and additional watering.	26
12. X-ray absorption spectra changes due to oxidation.....	28
13. Sequence for data collection at SSRL.	29
14. Microprobe image of the contaminated layer.....	30
15. X-ray absorption near edge structure (XANES) spectra of selected As standards.....	31
16. X-ray absorption near edge structure (XANES) spectra of selected elevated As locations.....	32
17. Line scans were collected at APS.....	34

CHAPTER I

INTRODUCTION

Since 2001, when the United States Environmental Protection Agency (EPA) passed stricter regulations on arsenic in drinking water reducing allowable concentrations from 50 to 10 $\mu\text{g/L}$, more attention has been brought to the agricultural feeding practices of poultry and swine. In particular, 3-nitro 4-hydroxyphenylarsonic acid or Roxarsone (ROX) (Figure 1) is used as a supplemental additive in poultry feed. ROX is an organoarsenic compound first introduced to feed in the 1940s in order to increase weight gain, feeding efficiency (ratio of feed eaten to slaughter weight), and to control pigmentation and coccidial intestinal parasites (Han *et al.*, 2004; Nachman *et al.*, 2005; Cortinas *et al.*, 2006; Jackson *et al.*, 2006; Nachman *et al.*, 2008). The majority of arsenic is excreted into the litter (Morrison, 1969) but with more attention on arsenic poisoning, concern has been growing over the levels contained in tissue and meat (Lasky *et al.*, 2004; Wallinga, 2006).

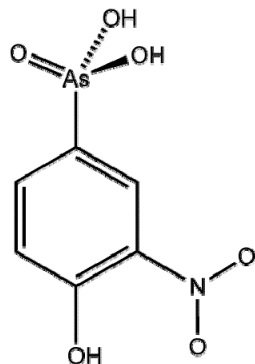


Figure 1. Chemical structure of roxarsone

1.1. Arsenic in Poultry Litter

According to the Poultry – Production and Value 2007 Summary Report (NASS, 2008) there were 8.9 billion broilers (baby chickens) produced in the U.S (~7% increase since 1996). If the average bird produces up to 4.9 kg of waste in its 48-day lifetime (ASAE, 2005) the annual production would be 44 billion kilograms of waste. Using the 2007 production census to update Garbarino *et al.* (2003), while retaining their assumptions that only 70% are treated with ROX and each broiler excretes 150 mg of ROX, it would result in 9.3×10^5 kg of ROX or 2.7×10^5 kg As. With this increase in poultry production, along with decreasing numbers of farms, the problems associated with disposal of litter waste in concentrated areas are growing. The current practice is land application for fertilizer, while other uses are slowly coming online, such as biomass-fueled power plants and pelletization (Nachman *et al.*, 2008).

Poultry manure typically contains 30 to 77 ppm As (Jackson *et al.*, 2003); however, composting manure, the typical practice throughout the winter months, may cause increases in As concentration due to the amount of water and carbon dioxide lost. This loss decreases the litter weight by 40 to 80%, increasing As concentrations between 50 and 500% (Bellows, 2005).

Prior studies have shown that As in poultry litter is at least 70-90% water-soluble (Garbarino *et al.*, 2003). When broilers are fed ROX-supplemented feed, the litter contains 36 to 88% of the total arsenic as unaltered ROX. The remaining As is mostly inorganic arsenate (As(V)), with minor traces of dimethylarsinic acid (DMA(V)) and unidentified As species resulting from degradation of ROX (Garbarino *et al.*, 2003). Degradation of litter applied to agriculture fields continues producing the more toxic and

mobile inorganic arsenic species arsenite (As(III)) and arsenate (As(V)), depending on the pH and redox conditions (Figure 2).

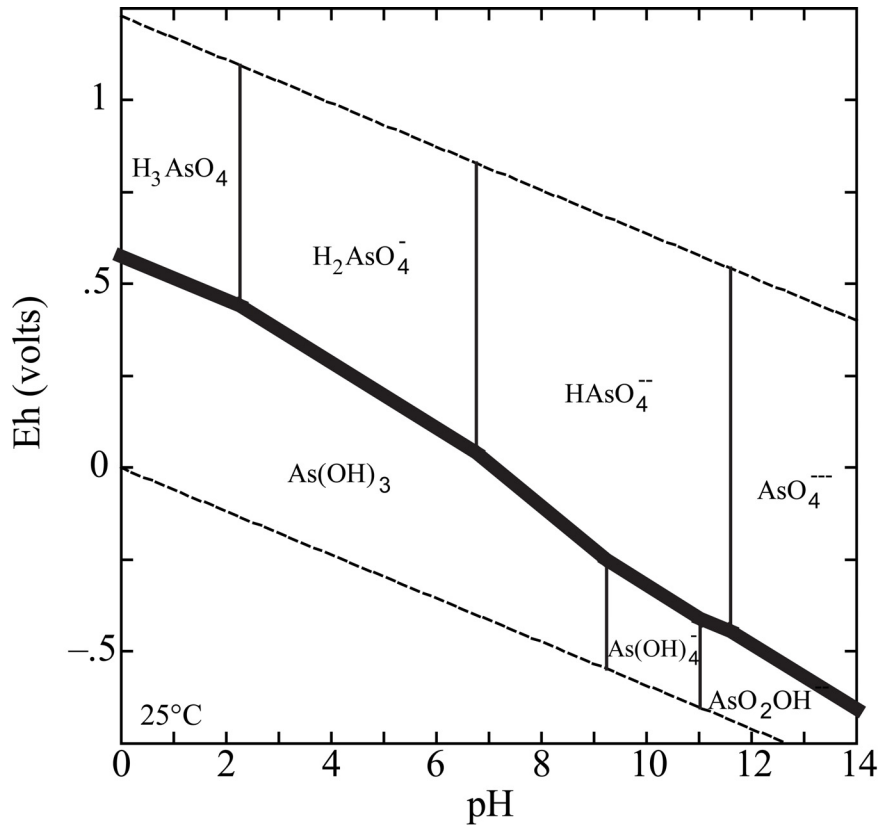


Figure 2. Thermodynamic stability fields for As compounds, in the system As-O-H at 25°C, 1 atm. Compounds below heavy black line are As(III); above are As(V).

1.2. Arsenic Toxicity

After the inadvertent exposure of millions of people to arsenic from drinking groundwater in Asia (e.g. van Geen *et al.*, 2006; Nickson *et al.*, 2000; Berg *et al.*, 2001), the knowledge base of arsenic as a toxin has become increasingly established. In dose-response terms, arsenic has beneficial usages at low dosages (e.g. Chen *et al.*, 1997; Wang *et al.*, 2004); however, high doses can result in adverse health conditions such as

cancer, cardiovascular disease, diabetes, skin lesions, and death (e.g. Abernathy *et al.*, 1999; Hughes, 2002; Silbergeld and Nachman, 2008). Yet, while an expanse of studies have documented the effects of arsenic once it is ingested, information on biogeochemical controls of As mobility and transformation in soil is key to understanding As toxicity, mobility, and bioavailability, as they are results of As oxidation state, speciation, and local microenvironments (Foster *et al.*, 1998).

Until recently, it was generally accepted that inorganic species, As(III) more so than As(V), are more toxic than organic species. Newer research suggests that methylated varieties of As(III) can be as toxic as the inorganic As(III) and more toxic than methylated varieties of As(V) (Styblo *et al.*, 1997; Styblo *et al.*, 2000). Methylated varieties of As(V), even though they are considered less toxic, may potentially serve as cancer promoters (Brown *et al.*, 1997) and are carcinogenic in animal experiments (Kenyon and Hughes, 2001). Regardless of speciation, adverse health effects may result from exposure to As; therefore, it is important to understand the environmental controls that control the mobility and transformation of As, especially from anthropogenic sources such as ROX-bearing poultry litter.

1.3. Earthworms

Since Darwin's study of earthworms in 1838, scientists have agreed that they remove debris from the surface and incorporate it into the subsurface soils as they burrow. In the proposed study, *Lumbricus terrestris* is used to characterize the increase in macroporosity of the soil and the distribution of As within the burrow walls and with depth resulting from earthworm burrowing. *L. terrestris*, the common night crawler, is

ideal since it is classified as a litter consumer and an anecic earthworm, meaning it uses the same burrow continuously, compacting and reinforcing the wall (Perreault and Whalen, 2006; Bernier, 1998). The earthworm reinforces the burrow by incorporating organic matter (OM) into the soil using mucus secretions as a strengthening agent (Edwards and Shipitalo, 1998).

Darwin estimated, after three decades of watching his flagstone path sink and disappear underground, that worms bring more than 10 tons of soil per acre per year to the surface, 2.4×10^{-3} ton per m^2 per year, and incorporate new surface litter into the subsurface (Baskin, 2005). Gabet *et al.* (2003) estimated volumetric soil movement between 5.4×10^{-4} - $0.01 \text{ m}^3 \text{ m}^{-2} \text{ yr}^{-1}$, varying among species. *L. terrestris* feeds 10-15 cm from its' burrow openings to collect debris that it incorporates along the burrow wall to depths of 1-3 m (Armourchelu and Andrews, 1994). Jégou *et al.* (1998) reported that the *L. terrestris* only made two or three burrows compared to the more numerous burrows observed from other species.

Earthworms, in particular anecic species such as *L. terrestris*, cause significant OM turnover (Devliegher and Verstraete, 1997; Marhan and Scheu, 2005). Jégou *et al.* (1998) compared four different species of earthworms' incorporation of OM into the drilosphere, the part of soil influenced by earthworm secretion and cast material, ~2 mm surrounding the burrow wall. Rye litter was applied to the surface to provide a controlled amount of OM. The total organic carbon analyzed from the burrow wall of *L. terrestris* was composed of 45% litter at all depths, as a result of continual usage. It is suggested that *L. terrestris* deposit casts (fecal matter) into the burrows; later, it is incorporated into the walls, causing the increase in OM (Tiunov and Scheu, 1999).

Earthworms are responsible for contaminant redistribution caused by burrowing activity and the production of macropores (Farenhorst *et al.*, 2000; Zorn *et al.*, 2005a and b; Binet *et al.*, 2006). *L. terrestris* were responsible for a significant increase in zinc concentrations of non-polluted soil from a buried contaminated layer in a column experiment compared to control columns. Zinc concentrations at the surface were also increased by the cast material deposited by the worm. Evidence from this study shows that *L. terrestris* are not only responsible for redistributing the contaminant at depth, but also transport contaminants from depth to the surface (Zorn *et al.*, 2005a).

L. terrestris is classified as a compacting worm as it continually uses the same burrow and packs the walls with OM. Bastardie *et al.* (2005) demonstrated that *L. terrestris* indeed compact the burrow walls by comparing the soil densities of artificial burrows with *L. terrestris* burrows. Due to the compaction, the diffusion of water into *L. terrestris* burrows walls was less than that of the artificial burrow, resulting in macropore structures that serve as preferential flow paths.

Soil macropores such as cracks and burrows have been studied to determine rainwater and irrigation infiltration rates. Both Shipitalo and Gibbs (2000) and Shipitalo *et al.* (2004) examined the interactions between tile drainage systems that promote the removal of excess subsurface water and *L. terrestris* burrows, and suggest that the infiltration rate was increased under saturated conditions because the burrows allowed water to drain quickly to the tiles. Similar projects have showed increased infiltration under a variety of different agricultural tillage practices when *L. terrestris* is present. No-till conservation practice (little to no soil disruption between growing seasons) allows the *L. terrestris* to establish burrows over a longer time resulting in a higher infiltration rate

(Lachnicht *et al.*, 1997; Willoughby *et al.*, 1997; and Willoughby and Kladivko, 2002). In contrast, other tillage practices disrupt the upper portion of the soil, disconnecting burrows from the surface (Willoughby *et al.*, 1997; Willoughby and Kladivko, 2002).

1.4. Study Scope

The first objective of this study was to provide a better estimate of bioturbation rate for *L. terrestris* and determine the role that burrows play in contaminant transport. Mesocosms were constructed using artificial soil, each containing a layer mixed with ROX to obtain 85 ppm As. Experimental data from water-soluble As extractions of soil in constructed mesocosms were fit by adjusting parameters in a theoretical model developed to simulate bioadvection and biodiffusion. The second objective was to determine the potential for redistribution and biotransformation of As due to the interaction with earthworms. *In situ* analyses of mesocosm soils provided key evidence aimed at As speciation, providing a better understanding on mobility and potential bioavailability to higher organisms.

CHAPTER II

MATERIALS AND METHODS

2.1. Artificial Soil

Artificial soil was made according to the Organization of Economic Cooperation and Development (OECD) for earthworm acute toxicity studies and contained 10% sphagnum peat moss (Les Tourbes Niro), 20% kaolin clay (Sigma Aldrich, product code K7375, CAS# 1332-58-7), and 70% industrial sand (>50% particles between 50-200 microns, Quikrete) (OECD, 1984). A professional grade mixer (Univex SRM30+) was used in order to obtain a homogeneous soil. A portion of the homogenous soil was removed, mixed with roxarsone (Acros Organics, CAS# 121-19-7) in a separate container to obtain 85 ppm As, and rotated using a Rotamix (ATR Model 10101) at 85 rpm for three hours.

2.2. Mesocosm Construction

Experimental mesocosms were constructed from acrylic pipe (5 cm Ø) 34 cm long and filled to a depth of 30 cm with alternating layers described below. Fine fiberglass mesh covered both ends to retain the soil and earthworm. Soil was added according to Capowiez's compression method (2001) to ensure consistent compaction through the column. Mesocosms were suspended in a wood box to simulate burial and lighting was controlled in 12-hr light-dark cycles using a full spectrum natural light for the duration of the experiments (Figure 3).



Figure 3. Experimental setup for mesocosm studies. To simulate burial, columns were hung level to soil surface and the lower portion of the wood box was covered in dark plastic to shield from light. Light was controlled in 12-hr light/dark cycles with a full spectrum light attached to the top of the box.

L. terrestris were obtained locally (DMF Bait Co) and classification was verified using the taxonomic key developed by Worm Watch (2000). Earthworms were stored in a large container with a mixture of peat moss and sand until needed. Prior to introduction into columns, earthworms were washed off, patted dry and weighed.

2.3. Bioturbation Columns

To explore the *L. terrestris* burrowing effect on vertical As transport, mesocosms were constructed as described in Section 2.2. In this group the ROX contaminated soil was 1 cm in thickness, located 5-6 cm from the surface (Figure 4A). Four groups of columns were constructed to compare the effects of burrowing and the addition of water. One worm per column was introduced and monitored daily to observe surface cast

production; worms were replaced after two days of no activity. Initial soil moisture of all columns was 30%.

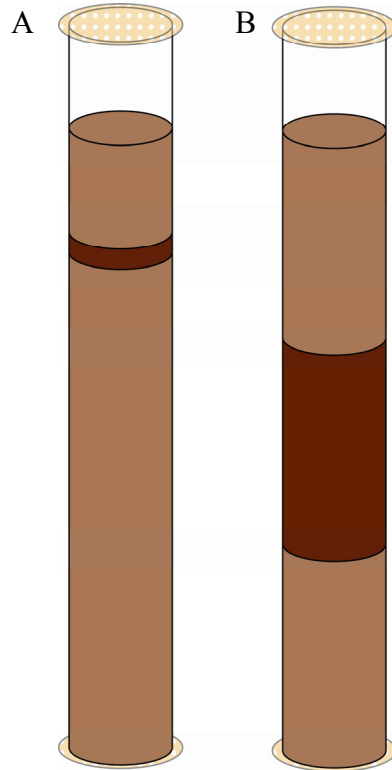


Figure 4. Mesocosm designs for column experiments to determine vertical As redistribution (A) and As speciation and mobility (B). Columns were filled with 30 cm of artificial soil containing fine-grained sand, kaolin clay, and peat moss. Contaminated layers, shown in dark brown, contained 85 ppm As as ROX and were 1 (A) and 10 (B) cm in thickness and at depths of 5-6 (A) and 10-20 (B) cm depth. Fiberglass mesh covered the ends of the columns to retain the soil and earthworm

Two groups had one addition of 10 ml of water during the 45 days, to promote burrowing activity. The other two groups were watered twice, 10 ml on the 16th day and 80 ml on the 35th day, equivalent to 0.6 and 5cm rainfall. All groups were given biweekly additions of peat moss at the surface. After the 45 days, columns were frozen in liquid nitrogen (LN₂) and cut into 1 cm sections (upper 16 cm) and 2 cm sections (16-

30 cm depth). Samples from each depth were used to determine the amount of water-soluble As in the bulk soil samples following the methods of Han *et al.* (2004) with minor changes. Extractions were analyzed with ICP-MS, as described in [Section 2.4]. For statistical analysis, each mesocosm group had six replicates. Biodiffusion modeling was completed using MatLab [see Chapter 3 Section 2.1]. An overview of the mesocosms used is provided in Table 1.

Table 1. Model Experiment Mesocosms

Group	Earthworms	Watering	Number of Columns Analyzed
1	Control		2
2	X		3
3		X	2
4	X	X	3

2.4. Arsenic Mobility and Speciation Columns

In order to explore relationships between the *L. terrestris* burrows and the mobility and speciation of arsenic, contaminated ROX soil was added to the middle 10 cm depth of the 30 cm column (Figure 4B). Duplicate columns (ROX 1 and ROX 2) were constructed, and one worm per column was introduced and replaced if no activity was seen as described above. After 30 days of worm burrowing, columns were frozen in LN₂, cut into 3-4 cm sections and dried overnight at 40°C. Soil sections were applied to glass slides using epoxy (Epo-Thin Epoxy, Buehler) and allowed to harden overnight. The excess soil was scraped from the glass slide. Thick-sections were then used for

elemental mapping of the drilosphere and surrounding bulk soil by synchrotron X-ray microprobe. Microbeam X-ray Absorption Near Edge Structure (μ XANES) was used to identify As oxidation states as described in [Section 2.6].

2.5. Inductively Coupled Plasma Mass Spectrometry (ICP-MS) Analysis

Water-extractable As was measured following the Han *et al.* (2004) method with minor changes. Soil sections were pulverized using mortar and pestle, placed in tubes (>35 ml soil in 50 ml tubes) and homogenized using an end-over-end mixer (Rotamix, ATR Model 10101) at 70 rpm for 2 hours. Once homogenized, 1.5 g of soil was placed into centrifuge tubes with 15 ml of Nanopure DI water and mixed for 30 minutes (Mistral Multi-Mixer, Lab-Line Instruments), centrifuged for 20 min at 3225 G (Thermo IEC Centra CL3R) and decanted. Samples were then prepared for ICP-MS analysis using a 100-fold dilution in Nanopure water (~9.8 ml), 50 μ l of Indium as an internal standard (10 mg/L In; Multi-element Internal Standard; Spex CertiPrep, INC), and 100 μ l of 12 N HNO₃ (Ultrex II, Baker #6901-05). Every 10 samples a duplicate sample was prepared, and every 25 samples blank and spiked samples were prepared. Blanks and spikes were prepared identical using the same procedures as for samples, with the addition of 100 μ l of As to spike samples (10-fold dilution of 50 mg/L As; Spike Sample Standard 1; Spex CertiPrep, Inc). Internal standard results indicated that sample preparation was consistent and acceptable (t-test, $P < 0.005$).

2.6. Synchrotron X-ray Microprobe and X-ray Absorption Spectra

X-ray microprobe analysis was completed at the Stanford Synchrotron Radiation Laboratory (SSRL) on beamline 2-3 and the Advanced Photon Source (APS) on beamline 20-BM-B at Argonne National Laboratory. Analysis was completed at ambient temperature and pressure in fluorescence and transmission modes using a Si(220) and Si(111) double-crystal monochromator to control the beamline energy at SSRL and APS, respectively. Monochromator calibration was completed using the first inflection point of arsenic K (SSRL) and gold L_{III} (APS) absorption edges of reference foils in transmission mode. Figure 5 provides a schematic of equipment and samples setup used at SSRL. APS setup was similar except the energy reference standard was in a different configuration.

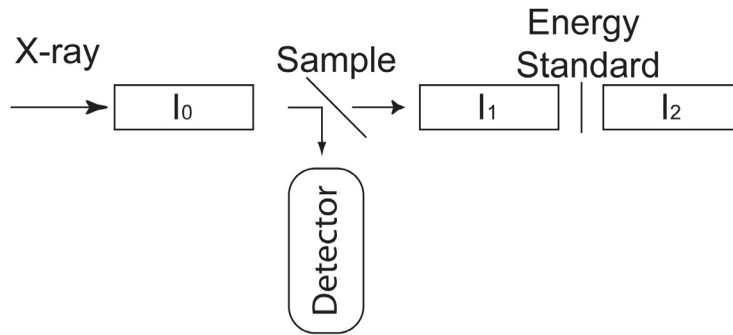


Figure 5. Representation of X-ray equipment setup used at SSRL. I_0 , I_1 , and I_2 represent ionization chambers filled with N_2 gas. Absorption spectrum for the sample is determined by the difference in X-ray intensity between I_0 and the detector, as the X-ray energy is controlled over a targeted energy range. The X-ray absorption energy edge positions of standards are determined by similar method using I_1 and I_2 .

Two different approaches were taken to locate positions of elevated As.

Microbeam X-ray fluorescence (μ XRF) elemental maps were collected at SSRL in order to provide locations of elevated As near the burrow and in the bulk soil. As K-edge

μ XANES spectra were then collected for selected spots in fluorescence mode over an energy range of 11635-12145 eV (ring condition: 3 GeV) using a Vortex detector.

The approach used at APS was to conduct “line scans” away from the burrow wall edge through the bulk soil. These scans provided possible locations of elevated As by continuous collection of fluorescence counts using a 13 element solid-state Ge fluorescence array detector. Scans provided intensity counts of As along lines across soil samples. As K-edge μ XANES spectra were then collected over an energy range of 11765-11920 eV (ring condition: 7 GeV) at selected locations.

CHAPTER III

EXPERIMENT 1: BIOTURBATION MESOCOSMS

3.1. Model Introduction

A common practice in describing solute transport through porous media is to use the classic one-dimensional advection-dispersion equation (ADE):

$$\frac{\partial C}{\partial t} = -\omega \frac{\partial C}{\partial z} + D \frac{\partial^2 C}{\partial z^2}. \quad (1)$$

Here C is the concentration of solute, t is time, z is the spatial position, ω is the advective speed, and D is the hydrodynamic dispersion coefficient. It is assumed that solute motion involves a random-walk process as water flows through the porous medium. As important as water movement is to the transport of contaminants, there are additional factors that must be addressed when considering the processes associated with biological transport and redistribution by bioturbation.

Biological mixing of sediment can be responsible for changes to physical, chemical, and biological properties (Boudreau, 1986; Wheatcroft *et al.*, 1990). Earthworms can be responsible for physical alterations through eating habits, consuming at the surface or at depth and excreting along burrow walls and the surface (e.g. Müller-Lemans and van Dorp, 1996; van den Bygaart *et al.*, 1998). Chemical alteration may take place due to production of mucus and by digestion and detoxification processes (e.g. Tiunov and Scheu, 1999; Langdon *et al.*, 2005; Watts *et al.* 2008). Biological alterations may also occur as environments suitable for microbial communities are produced in the

burrow, allowing for additional chemical alteration (e.g. Devliegher and Verstraete, 1997; Cortinas *et al.* 2006).

Biological transport and reworking of the soil leading to redistribution of tracers was suggested by Goldberg and Koide (1962) to be analogous to Fick's First Law of diffusion,

$$J = -D_B \frac{\partial C}{\partial z} \quad (2)$$

where J is the flux due to bioturbation and D_B is the proportionality constant, later described as the biodiffusion coefficient. This initial work was largely ignored until Guinasso and Schink (1975) first calculated biodiffusion coefficients (Boudreau, 1986). This initial model was quickly adopted in studies of deep-sea, near-shore, and lacustrine bioturbation, but was criticized for its simplicity and failure to address biological activity that resulted in advection movement. Below, the Fokker-Plank Equation (FPE) is developed in order to show that bioturbation can be modeled as a random walk process which includes advection movement, leading to what can be expressed as the ADE.

The result is two separate ADEs, one for aqueous flow and one for biological mixing, which are then combined to describe the results from the column experiments in this study. Therefore, it must be noted that values of ω and D_B represent a combination of biological and aqueous advection and diffusion/dispersion processes.

Due to the criticism of the initial model suggested by Goldberg and Koide, many models have been developed using different criteria. Meysman *et al.* (2003) compare these models and the criterion on which each was developed. Based on the general framework proposed to characterize the effects of bioturbation, models have been distinguished as discrete, semi-continuous, or continuous, and local or non-local. Local

means that the random walk of a particle is restricted to neighboring positions (i.e. particles can only move one length step at a time), whereas non-local means that a particle can move to any position within the domain of bioturbation during a small interval of time. Meysman *et al.* (2003) concluded that the main essential difference among models is whether motion is local or non-local. For simplicity of illustration the development below assumes local transport.

As models have been developed to clarify complexities of natural systems, additional factors have been incorporated within the ADE framework, notably how the biodiffusion coefficient D_B varies with depth, and effects of porosity and tracer retardation (e.g. Matisoff, 1982; Shull, 2001; Bunzl, 2002). The simplest assumption is that D_B is constant. The problem with this is that the activity of organisms may vary with depth, in which case D_B is not constant for the system. The issue then becomes whether D_B should be treated as varying either linearly, exponentially, or as a Gaussian function (Matisoff, 1982). An exponential variation was used in this study after the analysis of experimental data.

Most models have been developed for marine and lacustrine environments where porosity varies with depth. This may also apply in terrestrial settings, especially in agricultural fields, where the use of heavy equipment or the aeration process from tillage practices may both affect porosity. In this study, porosity is considered constant due to the construction of the columns to achieve similar porosity throughout the column (Capowiez *et al.*, 2001). Another factor included in some models is the retardation of the solute due to interactions with soil particles.

3.2. Methods

This section treats the physical redistribution of a contaminant (ROX in this study) resulting from bioturbation by earthworms. The development of the Fokker-Planck Equation (FPE) to express the redistribution of As throughout the experimental soil column is described. The aim is to illustrate how bioturbation, as a quasi-random process, involves both advective and diffusive components.

3.2.1. Development of Model

The movement of particles is treated as a Markovian process, where particles alternate between states of motion and rest. Details of motion are neglected, and each step has no influence on future particle movements. Let $f(z, t)$ denote the probability density that a particle is at position z at time t (Figure 6).

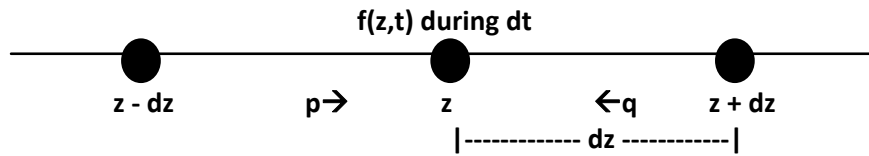


Figure 6. Schematic of random walk probability position.

During a small period of time, dt , the probability density is the additive result of the probability p that a particle moves a distance dz from the position $z - dz$ to z and the probability q that a particle moves a distance $-dz$ from $z + dz$ to z , such that

$$f(z, t + dt) = pf(z - dz, t) + qf(z + dz, t). \quad (3)$$

Expanding the term on the right side of (3) using a Taylor Series about z produces

$$f(z, t + dt) = p \left[f(z, t) - \frac{\partial f}{\partial z} dz + \frac{1}{2} \frac{\partial^2 f}{\partial z^2} (dz)^2 + \dots \right] \quad (4)$$

$$+ q \left[f(z, t) + \frac{\partial f}{\partial z} dz + \frac{1}{2} \frac{\partial^2 f}{\partial z^2} (dz)^2 + \dots \right].$$

By definition, $p + q = 1$, or $q = 1 - p$. Substituting this into (4) to eliminate q and rearranging,

$$f(z, t + dt) = p \left[f(z, t) - \frac{\partial f}{\partial z} dz + \frac{1}{2} \frac{\partial^2 f}{\partial z^2} (dz)^2 + \dots \right] \quad (5)$$

$$+ \left[f(z, t) + \frac{\partial f}{\partial z} dz + \frac{1}{2} \frac{\partial^2 f}{\partial z^2} (dz)^2 + \dots \right]$$

$$- p \left[f(z, t) + \frac{\partial f}{\partial z} dz + \frac{1}{2} \frac{\partial^2 f}{\partial z^2} (dz)^2 + \dots \right].$$

Factoring then yields

$$f(z, t + dt) = f(z, t) + (1 - 2p) \frac{\partial f}{\partial z} dz + \frac{1}{2} \frac{\partial^2 f}{\partial z^2} (dz)^2 + \dots \quad (6)$$

In turn the left side of (6) may be expanded as a Taylor Series with respect to time to give:

$$f(z, t + dt) = f(z, t) + \frac{\partial f}{\partial t} dt + \frac{1}{2} \frac{\partial^2 f}{\partial t^2} (dt)^2 + \dots \quad (7)$$

Combining (6) and (7) and rearranging then gives

$$\frac{\partial f}{\partial t} dt + \frac{1}{2} \frac{\partial^2 f}{\partial t^2} (dt)^2 + \dots = (1 - 2p) \frac{\partial f}{\partial z} dz + \frac{1}{2} \frac{\partial^2 f}{\partial z^2} (dz)^2 + \dots \quad (8)$$

Furthermore, dividing each side by dt and taking the limit as dt approaches zero produces

$$\lim_{dt \rightarrow 0} \left[\frac{\partial f}{\partial t} + \frac{1}{2} \frac{\partial^2 f}{\partial t^2} dt + \dots \right] = \lim_{dt \rightarrow 0} \left[(1-2p) \frac{\partial f}{\partial z} \frac{dz}{dt} + \frac{1}{2} \frac{\partial^2 f}{\partial z^2} \frac{(dz)^2}{dt} + \dots \right] \quad (9)$$

Assuming that the time and space steps are small, (9) may be truncated to second order to give

$$\frac{\partial f}{\partial t} = (1-2p) \frac{\partial f}{\partial z} \frac{dz}{dt} + \frac{1}{2} \frac{\partial^2 f}{\partial z^2} \frac{(dz)^2}{dt}. \quad (10)$$

This allows one to identify $\frac{dz^2}{dt}$ as the biodiffusivity coefficient D_B , and by definition

$(1-2p) \frac{dz}{dt}$ is the advection speed ω , so

$$\frac{\partial f}{\partial t} = -\omega \frac{\partial f}{\partial z} + \frac{1}{2} D_B \frac{\partial^2 f}{\partial z^2}. \quad (11)$$

which is the Fokker-Planck equation.

Letting N denote the total number of particles within the system, this constant may be incorporated within (11) such that

$$\frac{\partial}{\partial t} (Nf) = -\omega \frac{\partial}{\partial z} (Nf) + \frac{1}{2} D_B \frac{\partial^2}{\partial z^2} (Nf). \quad (12)$$

Furthermore, by definition $Nf(z,t)$ equals the number of particles per unit distance, n , at position z , so (12) becomes

$$\frac{\partial n}{\partial t} = -\omega \frac{\partial n}{\partial z} + \frac{1}{2} D_B \frac{\partial^2 n}{\partial z^2}. \quad (13)$$

In turn, multiplying this throughout by the (constant) particle mass converts (13) in terms of the concentration C , so

$$\frac{\partial C}{\partial t} = -\omega \frac{\partial C}{\partial z} + \frac{1}{2} D_B \frac{\partial^2 C}{\partial z^2}. \quad (14)$$

This development therefore illustrates that the effects of bioturbation, treated as involving quasi-random particle motions, can be described as an advection/diffusion process. A more general treatment (e.g. Risken, 1984) would lead to ω and D_B being within the differentials, in which case variations in ω and D_B can contribute to a particle flux. In this study, for simplicity it is assumed that the linear form of (14) is adequate to describe the effects of bioturbation. It is also important to point out that the effects of solute transport cannot be separated from the effects of bioturbation; therefore ω and D_B are additive from both processes.

Assuming that D_B does not vary rapidly over depth, then it can be calculated using a value D_o at the surface, with exponential decline with depth. The characteristic length scale (λ) is used to characterize the rate at which D_B changes with depth.

$$D_B = D_o * \exp\left(\frac{z}{\lambda}\right). \quad (15)$$

3.3. Results

3.3.1. Effects of Model Fit Values

The model coefficients and parameters (ω , D_o , and λ) were adjusted to fit the experimental data from the soil mesocosms, specifically, water-soluble As concentrations as a function of depth. Figure 7 shows the effect of varying each coefficient or parameter on the redistribution of As initially located in a 1 cm thick contaminated layer between 10 and 11 cm in depth. Advection (ω ; Figure 7A and B) and diffusion (D_o ; Figure 7C and D) are responsible for the position and spread of the contaminant, respectively. The smaller the value the smaller the shift or spread is from the initial condition. Advection

may also be negative, indicating a shift toward the surface, or positive, indicating a shift to greater depth. The characteristic length (λ) affects the exponential decay rate of D_0 . Small λ values result in a larger exponential decay (Figure 7E), while larger values result in a more normal redistribution (Figure 7F). Positive values result in decay with depth, while negative values decay towards the surface (not shown).

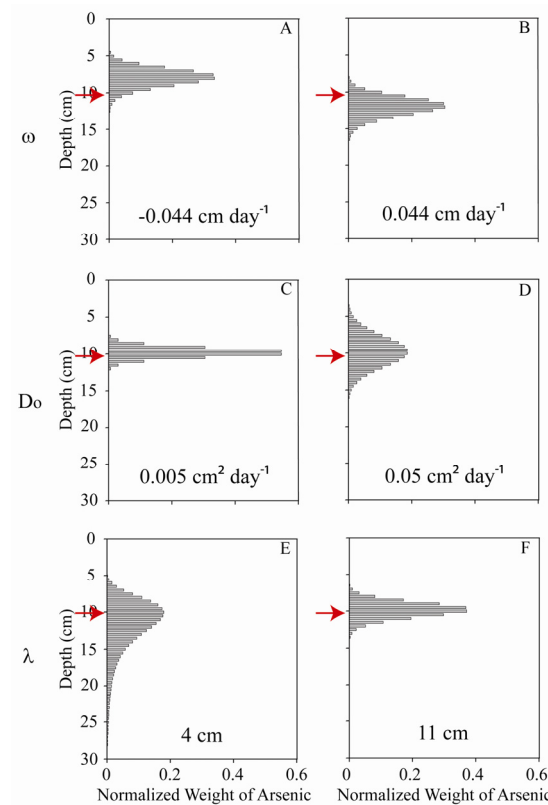


Figure 7. Effects of changing model fit values for an initial contamination layer 1 cm thick between 10 and 11 cm in depth (arrow). The advection coefficient (ω) affects the final peak position; when the value is negative peak position moves towards the surface (A) and when positive to greater depth (B). The diffusion coefficient (D_0) controls the spreading effect of the contamination. Small values result in minor spreading (C), while larger values increase spreading (D). The characteristic length-scale (λ) affects the exponential decay rate of D_0 . Small λ values result in a larger exponential decay (E), while larger values result in a more normal redistribution (F). Positive values result in decay with depth, while negative values decay towards the surface (not shown).

3.3.2. Without Worm or Added Water

Two control columns were used to determine the advection and dispersion terms associated with the initial addition of water to provide proper moisture content and the effects of drying on the dispersion aqueous control of As. Considering the two experimental data sets, the best fit was generated using values of $0.044 \text{ cm}\cdot\text{day}^{-1}$ and $0.029 \text{ cm}^2\cdot\text{day}^{-1}$ for advection and dispersion, respectively (Figure 8).

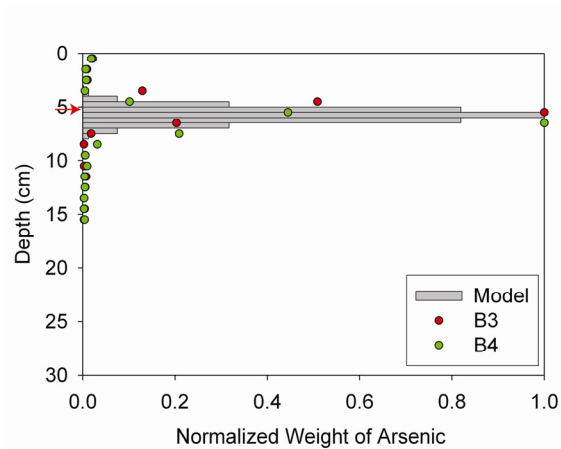


Figure 8. Control mesocosm model results. Model (grey histogram) was based on data averaged from two control columns (green and red dots). Initial moisture and drying resulted in a normal redistribution; diffusion was constant with depth so λ was not used in the model. Red arrow indicates location of the initial contaminated layer.

3.3.3. With Worm, Without Added Water

The columns containing worms but no additional water were modeled in order to understand the diffusion trends and determine the relative importance of advection caused by the worm. Earthworms burrowed to different depths in each column. Column A-2 (a) had a burrow depth of 8 cm, while A-3 (b) was similar at 7 cm depth; A-5 (c) provided a larger picture as the earthworm burrow extended almost half the depth of the column at 13 cm (Figure 9). Table 2 provides the advection (ω), initial diffusion (D_0),

and characteristic length-scale (λ) values of these experimental columns and the controls of both non-watered and watered columns.

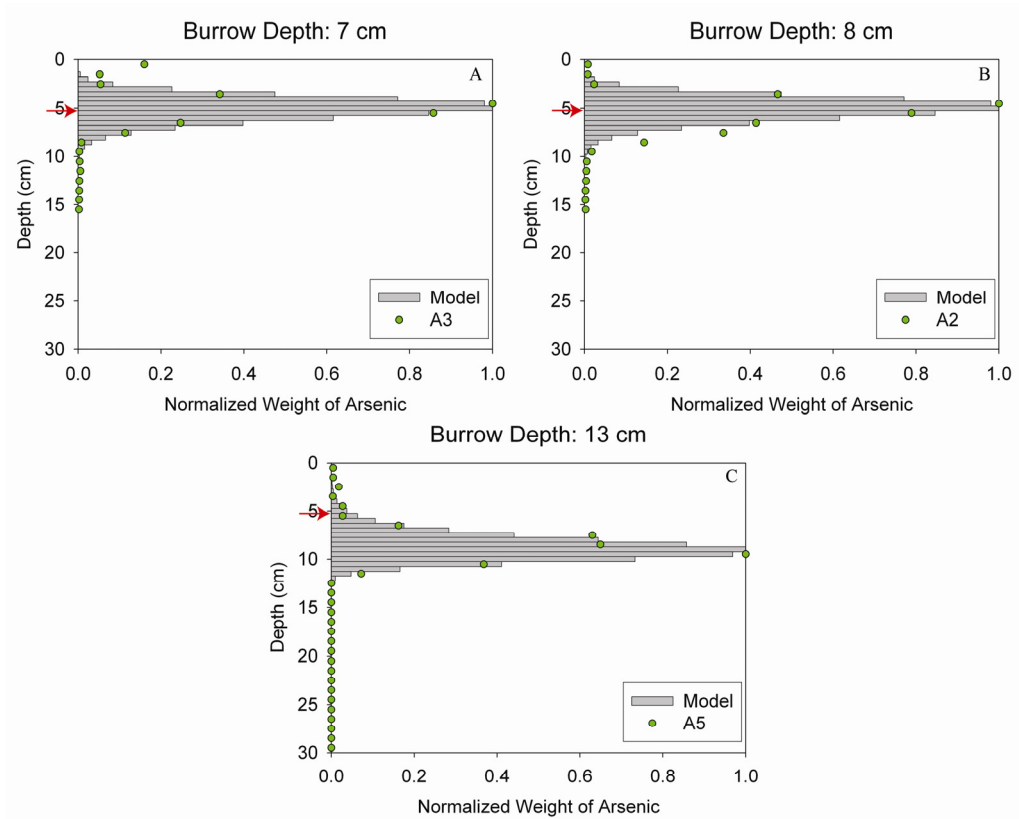


Figure 9. Earthworm bioturbation mesocosm model results (grey) compared to the water-extractable As experimental data (green). Shallow burrows (A and B) result in an overall upward movement of the contaminant, requiring a negative advection term (ω), while diffusion decayed with depth. Deeper burrows (C) cause an increase in contaminant concentration with depth (positive ω), and a decay towards the surface (negative λ) potentially resulting from more earthworm activity at depth. Red arrow indicates location of the initial contaminated layer.

3.3.4. With Added Water, Without Worm

Figure 10 displays the effect water has on the mobility of ROX and the distribution patterns associated with no burrowing activity. Unlike the distribution seen in previous figures the asymmetrical distribution is downward and was best modeled by an exponential dependence of D_B . Column D-1 (A) was best fit with values of 0.5

$\text{cm}\cdot\text{day}^{-1}$ for advection and initial dispersion of $0.0019 \text{ cm}^2\cdot\text{day}^{-1}$, while Column D-5 (B) had an advection of $0.667 \text{ cm}\cdot\text{day}^{-1}$ and initial dispersion of $0.0021 \text{ cm}^2\cdot\text{day}^{-1}$ (Figure 10).

Table 2. Model values used to fit experimental column data.

Watering		Earthworm		
		No	Yes	Yes
NO	Burrow Depth (cm)		7 - 8	13
	ω ($\text{cm}\cdot\text{day}^{-1}$)	+0.013	-0.011	+0.089
	D_0 ($\text{cm}^2\cdot\text{day}^{-1}$)	0.003	0.004-0.005	0.13
	λ (cm)	0	+5	-3
YES	Burrow Depth (cm)		7 - 9	12
	ω ($\text{cm}\cdot\text{day}^{-1}$)	+0.022	-	-
	D_0 ($\text{cm}^2\cdot\text{day}^{-1}$)	0.0015-0.019	-	-
	λ (cm)	+2.3	-	-

3.3.5. With Worm and Added Water

Figure 11 shows the ROX distribution as a result of the combination of watering and burrowing activities. The combined result of watering and burrowing resulted in significant As redistribution to depth in columns C4 (B) and C3 (C). Column C3 (C) was burrowed to a depth of 12 cm, while C4 (B) and C5 (A) had shallower burrow depths of 9 and 7 cm, respectively. However, C4 had an area between 2-4 cm where the worm had burrowed extensively, leaving a large void in the soil column. The model was not applied to these columns due to the complexity of the system; neither the advection nor the diffusion terms were estimated.

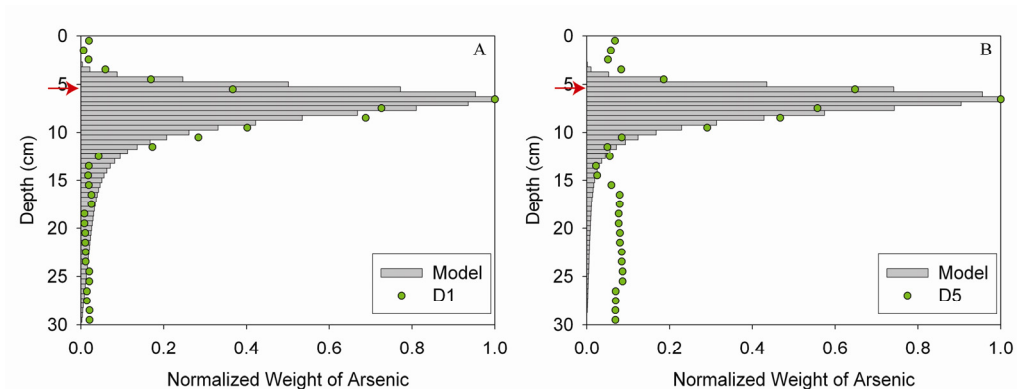


Figure 10. Aqueous control mesocosm model results support the initial assumption that As is water soluble in the columns, as it is transported to increasing depth. Red arrow indicates location of the initial contaminated layer.

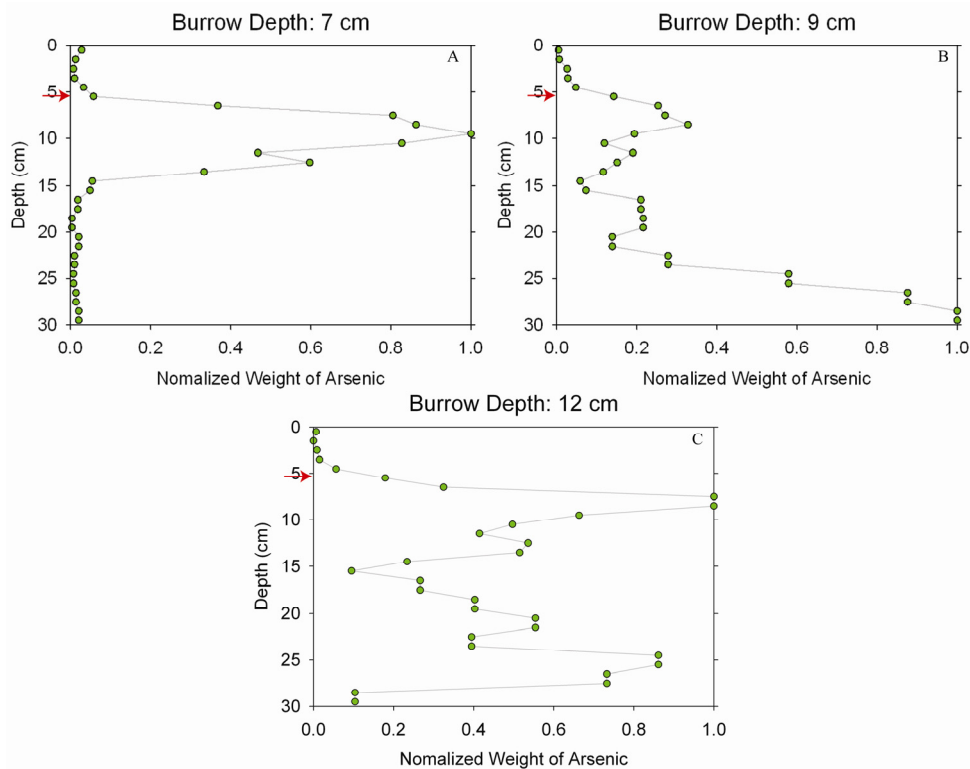


Figure 11. The combination of earthworm burrows and additional watering to simulate precipitation can result in significant As redistribution to depth. Shallow burrows (A & B) may have less effect in flushing the contaminant; however, larger voids caused by extensive burrowing (B) allow extensive flushing as do deeper burrows (C). Distribution models were not applied to these columns due to the complexity of the system. Red arrow indicates location of the initial contaminated layer.

CHAPTER IV

EXPERIMENT 2: ARSENIC MOBILITY AND SPECIATION MESOCOSMS

4.1. Synchrotron X-ray Absorption Spectroscopy (XAS)

Synchrotron radiation provides a continuous source of high intensity, highly collimated X-ray beams, greater than common laboratory X-ray sources. XAS provides information on atomic geometry and chemical state of absorbing atoms by providing an absorption spectrum that is related to the amount of energy required to eject a core electron, interacting with neighboring atoms. XAS provides a means to analyze samples *in situ* to determine speciation and distribution within a sample, without the need for chemical extractions that could change the speciation or destroy the sample. The energy needed to excite a K-shell electron of As in its native form (As(0)) is ~11867 eV, producing a white-line peak at ~11868.5 eV. When As becomes more oxidized it requires more energy to eject the core electron to the outer orbit; as a result there is a peak shift reflecting the oxidation state of the sample (Figure 12).

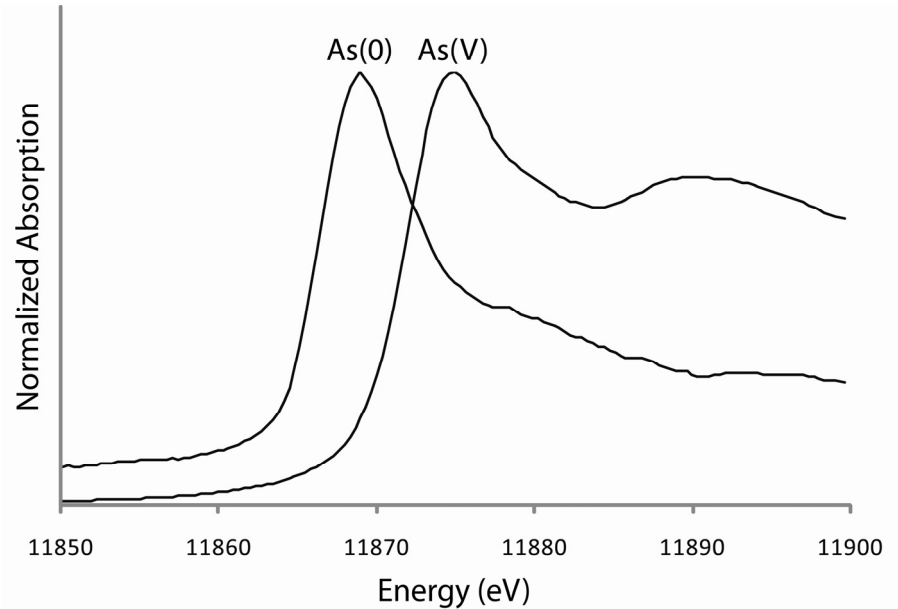


Figure 12. X-ray absorption spectra of As(0) and As(V) standards to show the effect of oxidation on peak position. More energy is required to eject the core electron from the oxidized species.

4.2. Microprobe Imaging Results

X-ray microprobe images collected at SSRL provided locations of elevated As concentrations. Figure 13 shows the typical sequence of data collection. The microprobe image (B) collected above the contaminated layer identifies areas of elevated As within close proximity to the burrow wall, and the blue area in the upper right corner is the burrow wall that does not elevated As at this location. The microprobe image of the contaminated layer (Figure 14) shows more dispersed areas of elevated As in contrast to the image collected above the contaminated layer. Again, the burrow wall is represented by the blue area at the top of the image.

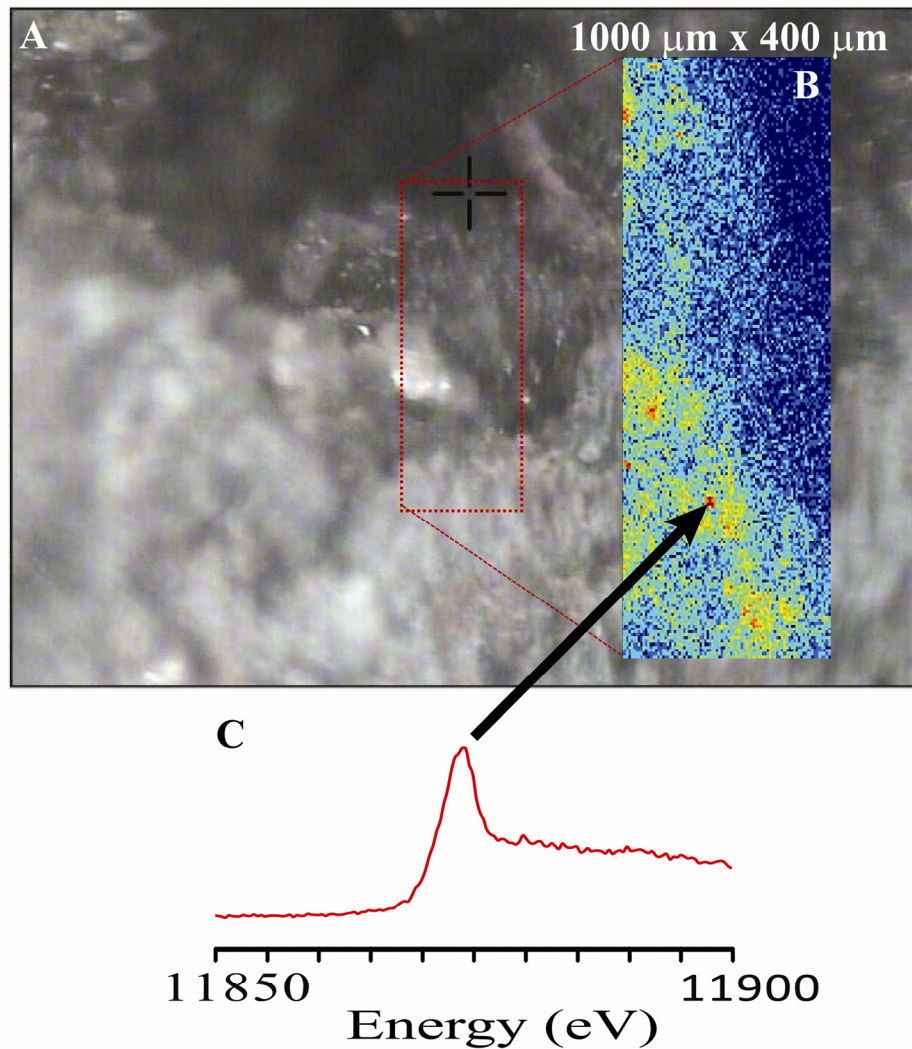


Figure 13. The sequence for data collection at SSRL was to identify an area of interest from the real-time imagery of the sample (A), located in this example at 9 cm in depth (above the initially contaminated layer). An X-ray fluorescence microprobe image was then collected (B) at the selected location. Images are in a cold-hot color scheme, where blue represents areas of low As concentration, while red represents areas of high As concentration. The microprobe image identifies areas of elevated As within close proximity to the burrow. The burrow wall (blue area in the upper right corner) does not show elevated As at this location. Microbeam X-ray absorption near edge structure spectra (C) were then collected on selected spots with elevated As.

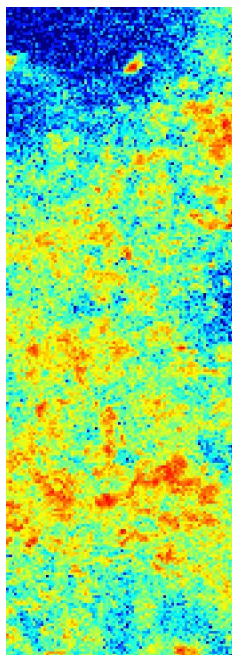


Figure 14. Microprobe image of the contaminated layer shows more dispersed areas of elevated As compared to the image collected above the contaminated layer (Figure 13). The image is in a cold-hot color scheme, where blue represents areas of low As concentration and red represents areas of high As concentration.

4.3. X-ray Absorption Near Edge Structure ANES Results

XANES spectra were collected from model compounds to compare to spectra of samples from experimental soil columns. Spectra for native As, sodium arsenate, and ROX standards were collected at SSRL, while As-Glutathione (Langdon *et al.*, 2002), DMA(V) (Smith, 2007), and As(III) salt (Webb *et al.*, 2003) were obtained from published sources (Figure 15). Figure 16 displays the XANES spectra from column 1 collected at both APS (1-6) and SSRL (1-0 (surface casts), 1-9, 1-16 worm, 1-12, and 1-22) [column number – depth (cm)]. Speciation change was observed along the vertical dimension of the burrow wall, but not horizontally through the drilosphere. Table 3 compares the “white-line” peak locations of standards to samples. The surface casts’ (1-

0) “white-line” peak location was at 11873 eV. Peak positions for 1-6, 1-9, and 1-22 are all located at ~11873 eV, while 1-12 was at 11874 eV. In contrast, the cross-sectional scan of the worm captured at 16 cm depth has its white-line peak at 11869 eV. The appearance of split peaks in some spectra appears in part due to low signal:noise ratio; this is apparent in samples 1-0, 1-9, 1-12, and 1-22. XANES spectra collected from the second column were similar to those from column 1, but due to low signal:noise ratio they are not shown.

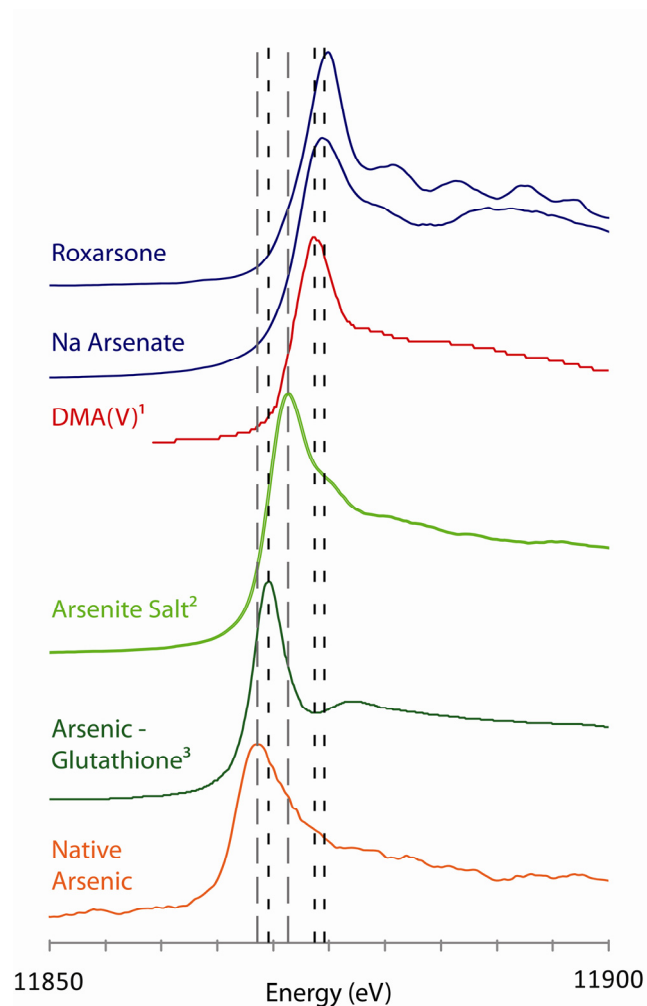


Figure 15. X-ray absorption near edge structure (XANES) spectra of selected As standards collected from SSRL (As(0), Sodium As(V), and ROX) and obtained from literature (¹Smith, 2007; ²Webb *et al.*, 2003; ³Langdon *et al.*, 2002).

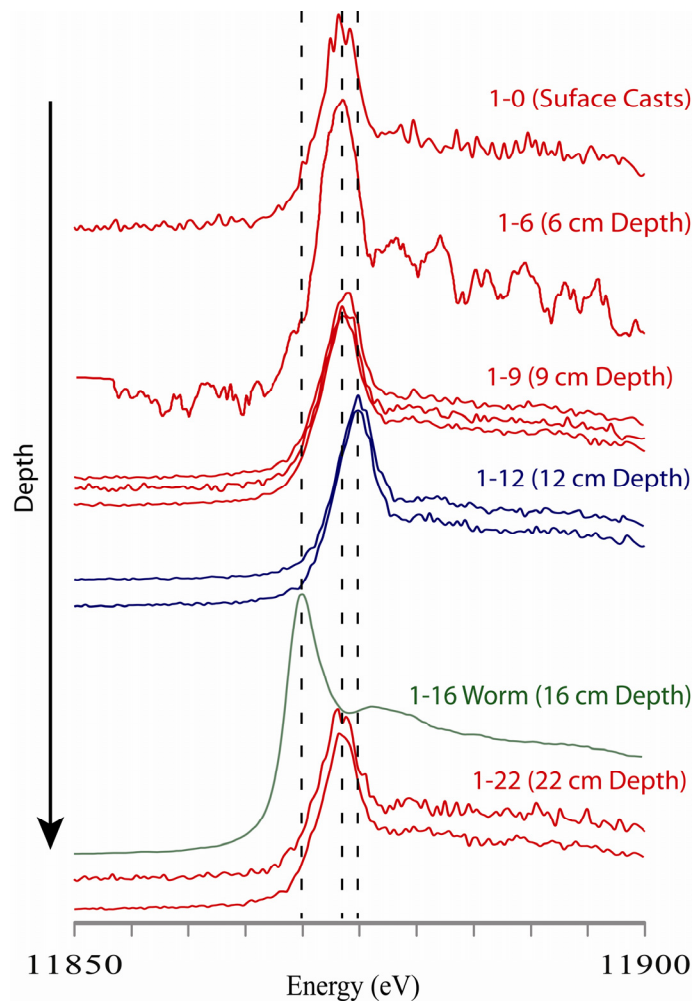


Figure 16. X-ray absorption near edge structure (XANES) spectra of selected elevated As locations on surface casts and along the drilosphere. Arsenic in all soil samples except the contaminated layer (12 cm depth) is in a methylated form (DMA(V)), while the contaminated layer is no longer ROX but an unidentified As(V) compound. In the earthworm tissue located at 16 cm depth, As has been reduced to As(III), likely as As-Glutathione.

4.4. Arsenic Redistribution

Line scans were collected at APS to determine locations where As was elevated in relation to the drilosphere. Vertical scans along the drilosphere were completed to assess potential evidence of As redistribution due to burrow activity. A set of scans collected

from 2~5 cm deep along the drilosphere displayed multiple areas of elevated As along the burrow wall above the initially contaminated regions (Figure 17 A).

Table 3. White-line Peak Positions of Standards and Experimental Samples

Standards			Experiment Samples		
	As Speciation	White-Line Peak		As Speciation	White-Line Peak
Roxarsone	As(V)	11874.5	Surface casts	DMA(V)	11873.5
Sodium Arsenate	As(V)	11874.5	6 cm	DMA(V)	11873.5
DMA(V)	As(V)	11873.5	9 cm	DMA(V)	11873.5
Arsenite salt	As(III)	11871	12 cm	As(V)	11874.5
Arsenic-Glutathione	As(III)	11869.5	Worm(16 cm)	Arsenic-Glutathione	11869.5
Native Arsenic	As(0)	11868	22 cm	DMA(V)	11873.5

Horizontal scans away from the burrow were completed at two depths to assess potential evidence of redistribution of As away from the drilosphere. Scans were completed at depths of 10 and 13 cm, denoted Rox 2-10 and 2-13, respectively. Scans of Rox 2-10 (above the contaminated region) display a higher concentration of As within the drilosphere, while there were only a few areas of higher concentration of As through the bulk soil to 1 cm away from the burrow wall (Figure 17 B). Rox 2-13 demonstrated elevated As at various locations through the bulk soil away from the burrow. No clear pattern was recognized, except that along the burrow wall of Rox 2-13 no elevated As was observed (Figure 17 C).

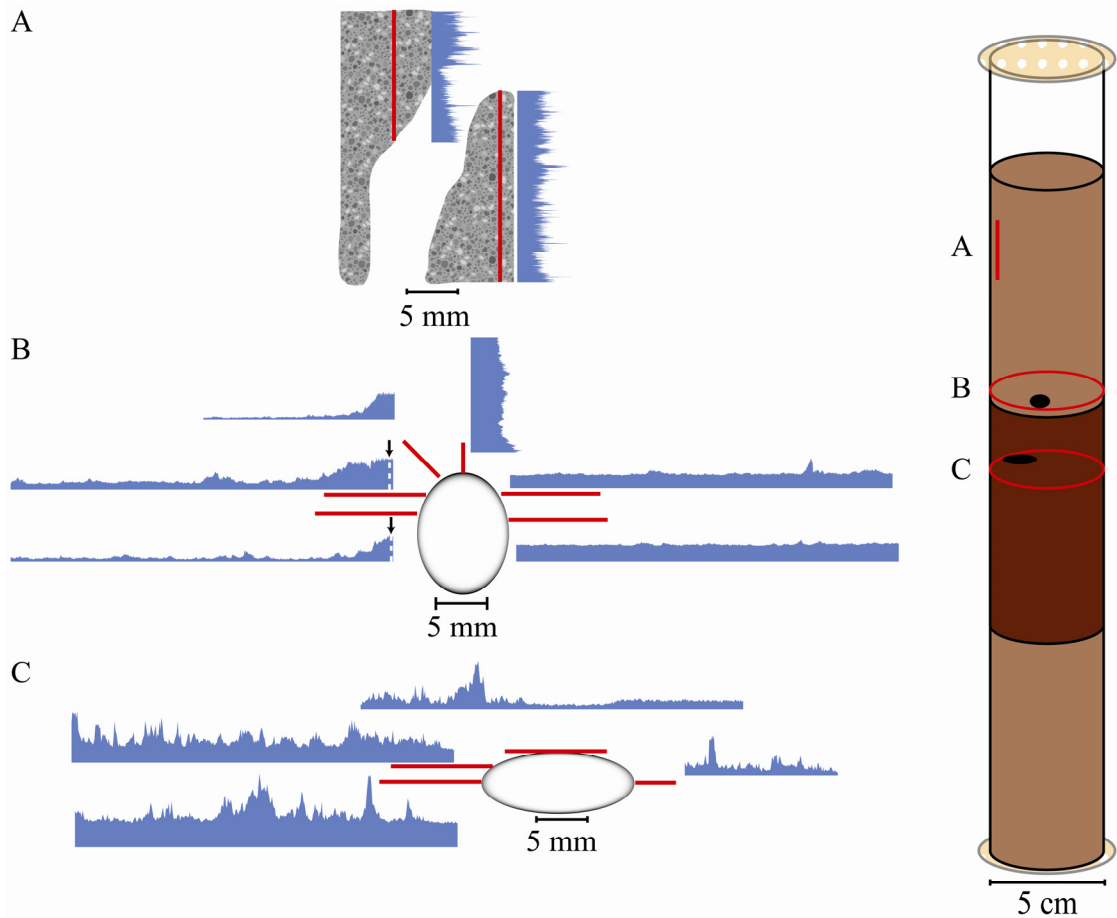


Figure 17. Line scans were collected at APS to determine locations of elevated As in relation to the burrow wall. Scans provided intensity counts of As along lines across the samples. Scans were collected along a vertical section of the burrow wall (A) and horizontal sections away from the burrow wall edge into the drilosphere (B and C). Locations of scan areas are indicated on the column diagram. Vertical scans display multiple areas of elevated As along the burrow wall. Horizontal scans above the layer of contamination (B) show multiple locations of elevated As near the burrow wall. The horizontal scans of the contaminated layer (C) demonstrated elevated As locations across the sample and a depletion of As along the burrow wall.

CHAPTER V

DISCUSSION

The mesocosm experiments described above (Ch. 3) have shown that bioturbation must be thought of not only as a diffusion process, but rather as an advection-diffusion process due to the feeding habits of *L. terrestris*. Another important issue that is brought up from the mesocosm experiments is the effect of biotransformation of arsenic (Ch. 4) and the potential to alter the mobility and bioaccessibility of As throughout the soil. The results from the laboratory study continue the effort to understand better the effects of bioturbation by earthworms on the mobility of contaminants, specifically arsenic.

5.1. Soil Mixing

5.1.1. Bioturbation Rates

The results from modeling the mesocosm experiments provide a better understanding of earthworm bioturbation rates. Prior work has examined the process of bioturbation using Cs distributions from the surface through the soil in order to provide an initial rate of consumption (van den Bygaart *et al.*, 1998). Others have calculated biodiffusion rates by measuring cast material brought to the surface (e.g. Müller-Lemans and van Dorp, 1996; Rodriguez, 2003; Zorn *et al.*, 2008). These calculations lead to conservative estimates of biodiffusion rates, as they do not take into account the amount of cast material that is incorporated into the burrow lining at depth (Lavelle, 1988). From this study, the use of columns and sampling As redistribution with depth allows for a

more accurate determination of bioturbation rates. Prior studies also refer only to a biodiffusion rate for *L. terrestris*, while this study shows the possibility that an advection process may play a key role in the redistribution. As shown in Table 2, rates for *L. terrestris* bioturbation vary with depth. Further work must be completed to assess accurately the potential of depth-dependent bioadvection and biodiffusion terms in order to provide improved biological modeling parameters.

5.1.2. Redistribution Potential

The potential for redistribution of As throughout the soil column is caused by a combination of two processes. The first is the physical redistribution due to the bioturbation process of the earthworm burrowing. This entails the physical displacement as the earthworms burrow through the contaminated layer as well as the ingestion/egestion during burrowing. The second process that leads to redistribution is the aqueous mobility of the contaminant, which depends on its chemical form.

5.1.2.1. Effects of Bioturbation

In the mesocosm experiments, high spatial resolution of earthworm bioturbation was obtained from the use of a 1 cm thick contaminated layer. This allowed the overall effect of bioturbation to be seen in a shorter time frame than in prior studies. Zorn *et al.* (2005a and b) used a thicker contaminated layer, delaying observable effects until after 80 days. Additional work needs to be accomplished to provide statistical analysis; however, this study provides evidence of possible trends. In general shallow burrows are responsible for upward movement of the contaminant, whereas deeper burrows result in

overall transport to depth. Even when burrows are deep, there is also a movement towards the surface, spreading what was a single contaminated layer throughout the upper portion of the soil column. These results are supported by the smaller-scale chemical analysis completed using synchrotron X-ray methods.

The burrow wall contained elevated levels of As above the contaminated layer, including surface casts, and below the contaminated layer (Figure 16). Horizontal line scans completed at APS [Section 2.6] provide evidence that earthworms are responsible for the movement of As in the columns as scans above the contaminated layer depict As only along the burrow wall and not in the bulk soil away from the burrow. There is also evidence of As removal from the contaminated layer, as the intensity of the X-ray fluorescence signal from As within the initially contaminated layer decreases along the burrow wall and increases in the bulk soil, whereas above the initially contaminated layer As is newly present along the burrow wall. This decrease in intensity is a result of As removal from the drilosphere of the contaminated layer by the earthworm; it is redistributed to areas above and below the contaminated layer.

5.1.2.2. Hydrologic Effects of Burrows

Previous studies have examined the association of earthworm burrows, infiltration rates, and field drain till effluents (e.g. Edwards *et al.*, 1990; Edwards *et al.*, 1992; Shipitalo and Gibbs, 2000; Shipitalo *et al.*, 2000). Collectively these studies have shown that earthworm burrows may serve as preferential flow paths allowing surface water to drain faster and to greater depths. Edwards *et al.* (1990) concluded that after 12 growing seasons with continuous no-till practices, 4% of rainfall flowed through the *L. terrestris*

burrows. The presence of the earthworm within the burrow has no significant impact on infiltration rates, allowing preferential flow even when earthworms are present in the burrow (Shipitalo and Butt, 1999).

The results of the mesocosm study support the idea of preferential flow paths as a means of transporting contaminants to greater depths, potentially contaminating ground water. Comparing Figures 10 and 11 shows that there is a significant difference in the redistribution of As caused by the presence of the burrows. The effect of bioturbation occurs in columns with or without watering (Figure 9 and 10); however, precipitation events when interacting with burrows allow for a greater distribution of As with depth.

5.1.3. Potential Outcomes of Bioturbation

The results of this study suggest two possible outcomes resulting from As redistribution in the presence of earthworms. During dry periods, earthworms are able to cycle As near the surface through dermal contact and ingestion, potentially resulting in an increase of bioaccessible As. In contrast, during precipitation events, burrows serve as preferential flow paths allowing water-soluble As to be transported to depth, potentially leading to ground water contamination. This study, along with previous studies, provides insight into potential outcomes of ROX-bearing poultry litter application in the presence of earthworms.

Through periods of little to no precipitation, bioturbation serves as the dominant mechanism of transport for contaminants. Langdon *et al.* (2003) explain that due to the intimate contact between soil and earthworm, interaction with As may be a result of dermal uptake or ingestion of either pore water, mineral fractions, or organic matter.

During deep burrowing activity, *L. terrestris* consumes organic matter at the surface, but also consumes a substantial amount of mineral soil at depth. The importance is that through ingestion, even As that is associated with another substance may enter the earthworm. Once ingested, As is readily biotransformed in order to protect the cells from arsenic toxicity (Langdon *et al.*, 2003). There is no known study suggesting how much of the consumed As is either bioconcentrated due to inability to remove it from the system or excreted as mucus, casts, or urine as organoarsenic compounds. Regardless, the results of this study demonstrate the ability to transport and biotransform As (the latter is discussed in Section 5.2).

Agricultural tillage practices are grouped as conventional or conservation tillage. Conventional tillage was commonly used in past decades to prepare fields after harvest for the following season. Conventional tillage removes plant material on the surface, and the disturbance of soil structure leads to an increase in soil erosion and surface run-off (Morgan, 1986). Over an extended period of time, hardpan layers form at a depth where tillage stops, creating a hydraulic barrier for water seepage (Shipitalo *et al.*, 2004). During the past few decades, rising interest in soil conservation has led to the adaption of conservation tillage practices. These practices reduce or eliminate the use of tillage after a harvest leaving plant residue at the surface. The decrease in soil disturbance modifies the soil structure resulting in a decrease in soil erosion rates. The plant residue provides soil nutrients and increases soil moisture (Morgan, 1986). Numerous studies have observed the effects tillage practices have on earthworm population and macropore transport (e.g. Lachnicht *et al.*, 1997; Malone *et al.*, 2003)

Through periods of precipitation, burrows may serve as preferential flow paths. Revisiting the characteristics of the *L. terrestris*, the continual use of the vertical burrow leads to compaction of the burrow walls. Through the process of ingestion/excretion, fine-grained particles are deposited along the burrow wall, decreasing the porosity over time (Jégou *et al.*, 2001). In agricultural settings, continuous no-till practices allowed 4% of precipitation to flow through the burrows (Edwards *et al.*, 1990). Shipitalo *et al.* (2004) examined the use of conventional tillage and determined that the plowed layer allowed for an increase in infiltration of the soil. Once the seeping water reached the base of the plowed layer, serving as a hydraulic barrier, water then moved laterally until a burrow opening was reached. Hence, regardless of tillage practices, earthworm burrows may serve as preferential flow paths allowing contaminants to reach greater depths.

5.2. Biotransformation and Degradation

The mesocosm study shows conclusively that biotransformation is taking place within the soil columns; however, from this study it is not known whether it is the earthworms or the potential presence of associated microbial communities, or both, that are responsible for the transformation. Langdon *et al.* (2003) proposed a metabolic pathway of arsenic through an earthworm from prior studies. Once ingested as either As(III) or As(V), various mechanisms reduce As(V) to As(III) (Irgolic, 1986). As(III)-thiol complexation occurs to S-rich proteins, such as glutathione (Morgan *et al.*, 1994; Yeates *et al.*, 1994; Langdon *et al.*, 2002). As(III)-thiol complexes are methylated to become organoarsenic compounds (e.g. arsenobetaine) (Langdon *et al.*, 2002). Organoarsenic compounds may be excreted through the mucus, casts, or urine.

5.2.1. Methylation along the Drilosphere

It is generally accepted that inorganic As(V) arsenate is the dominant arsenic species in aerobic bulk soils, and Fe-oxides serve as the dominant sink for As adsorption. Figure 16 shows that in the majority of locations with elevated As concentrations As was methylated into DMA(V), indicating the importance of biotransformation. Lafferty and Loeppert (2005) compared the sorption properties of methylated and inorganic arsenic species onto iron oxides. They concluded that DMA(V) is more mobile than As(V) and MMA(V) on iron oxide at pH 4 and 7, suggesting the adsorption affinity decreases as the degree of methylation increases.

In natural soil containing Fe-oxide, the biotransformation of As by earthworms from ROX (As(V)) to DMA(V) increases the mobility of As, and may potentially lead to an increase in bioavailability for plant uptake. Sadiq (1986) reported a significant correlation ($P < 0.05$) between As uptake in corn and water-extractable As. If the biotransformation of As(V) increases the water-extractable or mobile DMA(V), this potentially could lead to an increase in uptake by corn or other crops. Using HPLC-ICP-MS to determine speciation; Tlustos *et al.* (2002) reported that radish plants grown in soil amended with As(III), As(V), or DMA(V) showed that DMA(V) is detectable in both the roots and leaves, while As(III) is restricted to the roots and As(V) to the leaves. Unlike As(III) that oxidized to As(V), DMA(V) remained stable during their experiment. Water-extractions from the DMA(V) amended soils resulted in 70% DMA(V). The plants had a higher percentage of DMA(V) than the soil, suggesting radish plants can easily take up DMA(V) compared to inorganic As. Therefore, if As is readily biotransformed into

DMA(V) within the drilosphere, the resulting increases in mobility and bioavailability may potentially lead to an increase in uptake by plants.

5.2.2. Arsenic Speciation within Earthworm

XANES spectra collected from the earthworm cross-section suggest that As within the earthworm has been reduced to As(III) and bound to glutathione in agreement with previous studies (Morgan *et al.*, 1994; Langdon *et al.*, 2002; Landgon *et al.*, 2005). Extracts of earthworms have shown the presence of organoarsenic compounds such as arsenobetaine, DMA(V), and MMA, along with multiple arsenosugars (Geiszinger *et al.*, 1998; Geiszinger *et al.*, 2002). In this study, XANES spectra were only collected at one location on the earthworm; however, the previous studies' results suggest the As along the drilosphere was biotransformed and excreted by the earthworm.

CHAPTER VI

CONCLUSIONS AND IMPLICATIONS

The purpose of this research was to determine the effects of earthworm activity on the transport and biotransformation of ROX. The results of the modeling experiments show that bioturbation by *L. terrestris* is an advection-diffusion process. Modeling parameters were adjusted to fit experimental data to improve estimations of bioturbation rates; however, rates appear to be partially dependent on the depth to which an individual earthworm burrows. Further work needs to be completed to understand better the relationship of bioturbation rates to burrow depth. Earthworm burrows serving as macropores cause increased infiltration during precipitation events. Because *L. terrestris* burrow up to several meters in depth, the burrows provide potential pathways to contaminate ground water depending upon the speciation and mobility of As.

Synchrotron X-ray microprobe analyses of *in situ* soil samples along the drilosphere support the initial results from the modeling experiment that indicate As redistribution. Earthworms may deplete contaminants in soil through ingestion and dermal contact, redistributing them through egestion of casts or excretion of mucus. XANES analysis provides insight into the biotransformation of As through earthworm interactions as the As along the burrow was determined to be DMA(V), and within the earthworm, As-Glutathione.

As the poultry industry continues to grow in concentrated areas, the potential for increasing arsenic contamination must be addressed due to the use of ROX as a feed

additive. Due to the large push for soil conservation, no-till practices have become a typical method in agricultural settings. No-till practices allow earthworm populations to increase and their burrows to become more permanent with little to no disturbance.

Results from this study suggest that DMA(V) may be a more dominant species within the drilosphere than previously considered. Future work needs to address the potential of DMA(V) uptake in plants grown within the vicinity of earthworm burrows. Results of this research, along with results from prior studies (Tlustos *et al.*, 2002; Lafferty and Loeppert, 2005), suggest that as earthworms biotransform ROX into DMA(V), adsorption affinity decreases as methylation occurs. DMA(V) within the rhizosphere of some plants, may be readily adsorbed and transported within the roots and leaf tissues.

APPENDIX A

MATLAB MODEL CODE

```
%Earthworm Bioturbation Model
%Finite-Difference Solution of One-Dimensional
%Advection Diffusion Equation
%Written by David Furbish, Aaron Covey
%Last Modified Sept. 12, 2008

%Parameters
dx = 0.5; % space interval
dt = 0.0001; % time interval, day
N = 61; % number of nodes
Nt = 450000; % number of time steps
D0 = 0.005; % cm^2/day
lambda = 4; % Characteristic length scale variable to burrow depth

XX = (N-1)*dx; %total column distance

%Initial conditions
for i=1:N % set distances x
    x(i) = (i-1)*dx;
end

cold(1) = 0; % left boundary (node) condition
cold(N) = 0; % right boundary (node) condition

% Initialized Concentration Loop
for i=1:N % set initial interior node values
    cold(i) = 0;
end

for i=20:21
    cold(i) = 1; %****Initial Concentration, Normalized to 1
end

V = 0; % initialize video counter

for i=1:N-1
    D(i) = D0*exp((x(i)/lambda)); %exponential
end
```

```

%Diffusion Steps
for k=1:Nt % step through time
    for i=2:N-1 % step through space
        cnew(i) = cold(i) + (D(i)*dt/(dx^2))*(cold(i+1) - 2*cold(i) + cold(i-1));
    end

    for i=2:N-1
        temp(i) = cnew(i);
    end

%Advection Steps
tempA=mod(k,460000);
if tempA==0
    for i=2:N-1
        cnew(i)=temp(i-1);
    end
end

%Replace cold with cnew
for i=2:N-1 % set old values to with new values
    cold(i) = cnew(i);
end

%Create movie
tempV = mod(k,10000);
if tempV == 0
    V = V + 1;
    plot(x,cold);
    axis([0,30,0,1]);
    Mov(V) = getframe;
end
end

```

REFERENCES

- Abernathy, C. O., Liu, Y. P., Longfellow, D., Aposhian, H. V., Beck, B., Fowler, B., Goyer, R., Menzer, R., Rossman, T., Thompson, C., and Waalkes, M., 1999. Arsenic: Health Effects, Mechanisms of Actions, and Research Issues. *Environmental Health Perspectives* **107**, 593-597.
- Armourchelu, M. and Andrews, P., 1994. Some Effects of Bioturbation by Earthworms (Oligochaeta) on Archaeological Sites. *Journal of Archaeological Science* **21**, 433-443.
- ASAE (American Society of Agricultural Engineers), 2005. Manure Production and Characteristics - ASAE Standard D384.2. ASAE, St. Joseph, MI.
- Baskin, Y., 2005. *Under Ground: How Creatures of Mud and Dirt Shape Our World*. Island Press/Shearwater Books.
- Bastardie, F., Ruy, S., and Cluzeau, D., 2005. Assessment of Earthworm Contribution to Soil Hydrology: A Laboratory Method to Measure Water Diffusion Through Burrow Walls. *Biology and Fertility of Soils* **41**, 124.
- Bellows, B. C., 2005. Arsenic, Poultry Litter, and Organic Production Regulations: A Literature Review. *Abstracts of Papers American Chemical Society* **229**, U72-U73.
- Berg, M., Tran, H. C., Nguyen, T. C., Pham, H. V., Schertenleib, R., and Giger, W., 2001. Arsenic Contamination of Groundwater and Drinking Water in Vietnam: A Human Health Threat. *Environmental Science & Technology* **35**, 2621-2626.
- Bernier, N., 1998. Earthworm Feeding Activity and Development of the Humus Profile. *Biology and Fertility of Soils* **26**, 215.
- Binet, F., Kersanté, A., Munier Lamy, C., Le Bayon, R. C., Belgy, M. J., and Shipitalo, M. J., 2006. Lumbricid Macrofauna Alter Atrazine Mineralization and Sorption in a Silt Loam Soil. *Soil Biology and Biochemistry* **38**, 1255.
- Boudreau, B. P., 1986. Mathematics Of Tracer Mixing In Sediments: 1. Spatially-Dependent, Diffusive Mixing. *American Journal Of Science* **286**, 161-198.
- Brown, J., Kirk, T., and Kitchin, M., 1997. Dimethylarsinic Acid Treatment Alters Six Different Rat Biochemical Parameters: Relevance to Arsenic Carcinogenesis. *Teratogenesis, Carcinogenesis, and Mutagenesis* **17**, 71-84.

- Bunzl, K., 2002. Transport of Fallout Radiocesium in the Soil by Bioturbation: A Random Walk Model and Application to a Forest Soil with a High Abundance of Earthworms. *The Science of The Total Environment* **293**, 191-200.
- Capowiez, Y., Monestiez, P., and Belzunces, L., 2001. Burrow Systems Made by *Aporrectodea nocturna* and *Allolobophora chlorotica* in Artificial Cores: Morphological Differences and Effects of Interspecific Interactions. *Applied Soil Ecology* **16**, 109.
- Chen, G. Q., Shi, X. G., Tang, W., Xiong, S. M., Zhu, J., Cai, X., Han, Z. G., Ni, J. H., Shi, G. Y., Jia, P. M., Liu, M. M., He, K. L., Niu, C., Ma, J., Zhang, P., Zhang, T. D., Paul, P., Naoe, T., Kitamura, K., Miller, W., Waxman, S., Wang, Z. Y., de The, H., Chen, S. J., and Chen, Z., 1997. Use of Arsenic Trioxide (As₂O₃) in the Treatment of Acute Promyelocytic Leukemia (APL): I. As₂O₃ Exerts Dose-Dependent Dual Effects on APL Cells. *Blood* **89**, 3345-3353.
- Cortinas, I., Field, J. A., Kopplin, M., Garbarino, J. R., Gandolfi, A. J., and Sierra-Alvarez, R., 2006. Anaerobic Biotransformation of Roxarsone and Related N-Substituted Phenylarsonic Acids. *Environmental Science & Technology* **40**, 2951-2957.
- Devliegher, W. and Verstraete, W., 1997. Microorganisms and Soil Physico-Chemical Conditions in the Drilosphere of *Lumbricus terrestris*. *Soil Biology and Biochemistry* **29**, 1721.
- Edwards, W. M. and Shipitalo, M. J., 1998. Consequences of Earthworms in Agricultural Soils: Aggregation and Porosity. In: Edwards, C. A. (Ed.), *Earthworm Ecology*. CRC Press, Boca Raton, FL.
- Edwards, W. M., Shipitalo, M. J., Owens, L. B., and Norton, L. D., 1990. Effect of *Lumbricus terrestris* L. Burrows on Hydrology of Continuous No-Till Corn Fields. *Geoderma* **46**, 73.
- Edwards, W. M., Shipitalo, M. J., Traina, S. J., Edwards, C. A., and Owens, L. B., 1992. Role of *Lumbricus terrestris* (L.) Burrows on Quality of Infiltrating Water. *Soil Biology and Biochemistry* **24**, 1555.
- Farenhorst, A., Topp, E., Bowman, B. T., and Tomlin, A. D., 2000. Earthworm Burrowing and Feeding Activity and the Potential for Atrazine Transport by Preferential Flow. *Soil Biology and Biochemistry* **32**, 479.
- Foster, A. L., Brown, G. E., Tingle, T. N., and Parks, G. A., 1998. Quantitative Arsenic Speciation in Mine Tailings Using X-ray Absorption Spectroscopy. *American Mineralogist* **83**, 553-568.

- Gabet, E. J., Reichman, O. J., and Seabloom, E. W., 2003. The Effects of Bioturbation on Soil Processes and Sediment Transport. *Annual Review of Earth and Planetary Sciences* **31**, 249-273.
- Garbarino, J. R., Bednar, A. J., Rutherford, D. W., Beyer, R. S., and Wershaw, R. L., 2003. Environmental Fate of Roxarsone in Poultry Litter: I. Degradation of Roxarsone During Composting. *Environmental Science & Technology* **37**, 1509-1514.
- Geiszinger, A., Goessler, W., Kuehnelt, D., Francesconi, K., and Kosmus, W., 1998. Determination of Arsenic Compounds in Earthworms. *Environmental Science & Technology* **32**, 2238-2243.
- Geiszinger, A. E., Goessler, W., and Kosmus, W., 2002. Short Communication: An Arsenosugar as the Major Extractable Arsenical in the Earthworm *Lumbricus terrestris*. *Applied Organometallic Chemistry* **16**, 473-476.
- Goldberg, E. D. and Koide, M., 1962. Geochronological Studies of Deep Sea Sediments by the Ionium/Thorium Method. *Geochim. et Cosmochim. Acta; Vol: 26*, Pages: 417-50.
- Guinasso, N. L. and Schink, D. R., 1975. Quantitative Estimates of Biological Mixing Rates in Abyssal Sediments. *Journal of Geophysical Research* **80**, 3032-3043.
- Han, F. X., Kingery, W. L., Selim, H. M., Gerard, P. D., Cox, M. S., and Oldham, J. L., 2004. Arsenic Solubility and Distribution in Poultry Waste and Long-term Amended Soil. *Science Of The Total Environment* **320**, 51-61.
- Hughes, M. F., 2002. Arsenic Toxicity and Potential Mechanisms of Action. *Toxicology Letters* **133**, 1-16.
- Irgolic, K. J., 1986. Arsenic in the Environment. In: Xavier, A. V. (Ed.), *Frontiers in bioinorganic chemistry: International Conference on Bioinorganic Chemistry*. VCH: Weinheim, German; Deerfield Beach, FL.
- Jackson, B. P., Bertsch, P. M., Cabrera, M. L., Camberato, J. J., Seaman, J. C., and Wood, C. W., 2003. Trace Element Speciation in Poultry Litter. *J Environ Qual* **32**, 535-540.
- Jackson, B. P., Seaman, J. C., and Bertsch, P. M., 2006. Fate of Arsenic Compounds in Poultry Litter Upon Land Application. *Chemosphere* **65**, 2028.
- Jégou, D., Cluzeau, D., Balesdent, J., and Tréhen, P., 1998. Effects of Four Ecological Categories of Earthworms on Carbon Transfer in Soil. *Applied Soil Ecology* **9**, 249.

- Jégou, D., Schrader, S., Diestel, H., and Cluzeau, D., 2001. Morphological, Physical and Biochemical Characteristics of Burrow Walls Formed by Earthworms. *Applied Soil Ecology* **17**, 165.
- Kenyon, E. M. and Hughes, M. F., 2001. A Concise Review of the Toxicity and Carcinogenicity of Dimethylarsinic Acid. *Toxicology* **160**, 227.
- Lachnicht, S. L., Parmelee, R. W., McCartney, D., and Allen, M., 1997. Characteristics of Macroporosity in a Reduced Tillage Agroecosystem with Manipulated Earthworm Populations: Implications for Infiltration and Nutrient Transport. *Soil Biology and Biochemistry* **29**, 493.
- Lafferty, B. J. and Loeppert, R. H., 2005. Methyl Arsenic Adsorption and Desorption Behavior on Iron Oxides. *Environmental Science & Technology* **39**, 2120-2127.
- Langdon, C. J., Meharg, A. A., Feldmann, J., Balgar, T., Charnock, J., Farquhar, M., Pearce, T. G., Semple, K. T., and Cotter-Howells, J., 2002. Arsenic-Speciation in Arsenate-Resistant and Non-Resistant Populations of the Earthworm, *Lumbricus rubellus*. *Journal Of Environmental Monitoring* **4**, 603-608.
- Langdon, C. J., Pearce, T. G., Meharg, A. A., and Semple, K. T., 2003. Interactions Between Earthworms and Arsenic in the Soil Environment: A Review. *Environmental Pollution* **124**, 361.
- Langdon, C. J., Winters, C., St. Urzenbaum, S. R., Morgan, A. J., Charnock, J. M., Meharg, A. A., Pearce, T. G., Lee, P. H., and Semple, K. T., 2005. Ligand Arsenic Complexation and Immunoperoxidase Detection of Metallothionein in the Earthworm *Lumbricus rubellus* Inhabiting Arsenic-Rich Soil. *Environmental Science & Technology* **39**, 2042-2048.
- Lasky, T., Sun, W. Y., Kadry, A., and Hoffman, M. K., 2004. Mean Total Arsenic Concentrations in Chicken 1989-2000 and Estimated Exposures for Consumers of Chicken. *Environmental Health Perspectives* **112**, 18-21.
- Lavelle, P., 1988. Earthworm Activities and the Soil System. *Biology and Fertility of Soils* **6**, 237-251.
- Malone, R. W., Logsdon, S., Shipitalo, M. J., Weatherington-Rice, J., Ahuja, L., and Ma, L., 2003. Tillage Effect on Macroporosity and Herbicide Transport in Percolate. *Geoderma* **116**, 191.
- Marhan, S. and Scheu, S., 2005. Effects of Sand and Litter Availability on Organic Matter Decomposition in Soil and in Casts of *Lumbricus terrestris* L. *Geoderma* **128**, 155-166.

- Matisoff, G., 1982. Mathematical Models of Bioturbation. In: McCall, P. L. and Tevesz, M. J. S. Eds.), *Animal Sediment Relations*. Plenum Press, New York.
- Meysman, F. J. R., Boudreau, B. P., and Middelburg, J. J., 2003. Relations Between Local, Nonlocal, Discrete and Continuous Models of Bioturbation. *Journal of Marine Research* **61**, 391.
- Morgan, A. J., Winters, C., and Yarwood, A., 1994. Speed-Mapping Of Arsenic Distribution In The Tissues Of Earthworms Inhabiting Arsenious Soil. *Cell Biology International* **18**, 911-914.
- Morgan, R. P. C., 1986. *Soil Erosion and Conservation*. Longman, London.
- Morrison, J. L., 1969. Distribution Of Arsenic From Poultry Litter In Broiler Chickens, Soil, And Crops. *Journal Of Agricultural And Food Chemistry* **17**, 1288-&.
- Müller-Lemans, H. and van Dorp, F., 1996. Bioturbation as a Mechanism for Radionuclide Transport in Soil: Relevance of Earthworms. *Journal of Environmental Radioactivity* **31**, 7.
- Nachman, K. E., Graham, J. P., Price, L. B., and Silbergeld, E. K., 2005. Arsenic: A Roadblock to Potential Animal Waste Management Solutions. *Environmental Health Perspectives* **113**, 1123-1124.
- Nachman, K. E., Mihalic, J. N., Burke, T. A., and Geyh, A. S., 2008. Comparison of Arsenic Content in Pelletized Poultry House Waste and Biosolids Fertilizer. *Chemosphere* **71**, 500.
- NASS (National Agricultural Statistics Service), 2008. Poultry Production and Value 2007 Summary. United States Department of Agriculture, Washington D.C.
- Nickson, R. T., McArthur, J. M., Ravenscroft, P., Burgess, W. G., and Ahmed, K. M., 2000. Mechanism of Arsenic Release to Groundwater, Bangladesh and West Bengal. *Applied Geochemistry* **15**, 403.
- OECD, 1984. Guideline for Testing Chemicals No. 207 Earthworm, Acute Toxicity Tests. Organization for Economic Cooperation and Development, Paris, France.
- Perreault, J. M. and Whalen, J. K., 2006. Earthworm Burrowing in Laboratory Microcosms as Influenced by Soil Temperature and Moisture. *Pedobiologia* **50**, 397.
- Risken, H., 1984. *The Fokker-Planck Equation*. Springer-Verlag.
- Rodriguez, M. D., 2006. The Bioturbation Transport of Chemicals in Surface Soils. Master of Science, Louisiana State University.

- Sadiq, M., 1986. Solubility Relationships of Arsenic in Calcareous Soils and Its Uptake by Corn. *Plant and Soil* **91**, 241.
- Shipitalo, M. J. and Butt, K. R., 1999. Occupancy and Geometrical Properties of *Lumbricus terrestris* L Burrows Affecting Infiltration. *Pedobiologia* **43**, 782-794.
- Shipitalo, M. J., Dick, W. A., and Edwards, W. M., 2000. Conservation Tillage and Macropore Factors that Affect Water Movement and the Fate of Chemicals. *Soil and Tillage Research* **53**, 167.
- Shipitalo, M. J. and Gibbs, F., 2000. Potential of Earthworm Burrows to Transmit Injected Animal Wastes to Tile Drains. *Soil Sci Soc Am J* **64**, 2103-2109.
- Shipitalo, M. J., Nuutinen, V., and Butt, K. R., 2004. Interaction of Earthworm Burrows and Cracks in a Clayey, Subsurface-Drained, Soil. *Applied Soil Ecology* **26**, 209.
- Shull, D. H., 2001. Transition-Matrix Model of Bioturbation and Radionuclide Diagenesis. *Limnology and Oceanography* **46**, 905-916.
- Silbergeld, E. K. and Nachman, K., 2008. The Environmental and Public Health Risks Associated with Arsenical Use in Animal Feeds. *Annals of the New York Academy of Sciences* **1140**, 346.
- Smith, P. G., 2007. Arsenic Biotransformation in Terrestrial Organisms: A Study of the Transport and Transformation of Arsenic in Plants, Fungi, Fur and Feathers, Using Conventional Speciation Analysis and X-ray Absorption Spectroscopy. Doctorate of Philosophy, Queen's University.
- Stybło, M., Del Razo, L. M., Vega, L., Germolec, D. R., LeCluyse, E. L., Hamilton, G. A., Reed, W., Wang, C., Cullen, W. R., and Thomas, D. J., 2000. Comparative Toxicity of Trivalent and Pentavalent Inorganic and Methylated Arsenicals in Rat and Human Cells. *Archives of Toxicology* **74**, 289.
- Stybło, M., Serves, S. V., Cullen, W. R., and Thomas, D. J., 1997. Comparative Inhibition of Yeast Glutathione Reductase by Arsenicals and Arsenothiols. *Chemical Research in Toxicology* **10**, 27-33.
- Tiunov, A. V. and Scheu, S., 1999. Microbial Respiration, Biomass, Biovolume and Nutrient Status in Burrow Walls of *Lumbricus terrestris* L. (Lumbricidae). *Soil Biology and Biochemistry* **31**, 2039.
- Tlustoš, P., Goessler, W., Száková, J., and Balík, J., 2002. Arsenic Compounds in Leaves and Roots of Radish Grown in Soil Treated by Arsenite, Arsenate and Dimethylarsinic Acid. *Applied Organometallic Chemistry* **16**, 216-220.

- van den Bygaart, A. J., Protz, R., Tomlin, A. D., and Miller, J. J., 1998. ^{137}Cs as an Indicator of Earthworm Activity in Soils. *Applied Soil Ecology* **9**, 167.
- van Geen, A., Zheng, Y., Cheng, Z., He, Y., Dhar, R. K., Garnier, J. M., Rose, J., Seddique, A., Hoque, M. A., and Ahmed, K. M., 2006. Impact of Irrigating Rice Paddies with Groundwater Containing Arsenic in Bangladesh. *Science of the Total Environment* **367**, 769-777.
- Wallinga, D., 2006. Playing Chicken: Avoiding Arsenic in Your Meat.
- Wang, Z. W., Zhou, J., Lu, X. F., Gong, Z. L., and Le, X. C., 2004. Arsenic Speciation in Urine from Acute Promyelocytic Leukemia Patients Undergoing Arsenic Trioxide Treatment. *Chemical Research in Toxicology* **17**, 95-103.
- Watts, M. J., Button, M., Brewer, T. S., Jenkin, G. R. T., and Harrington, C. F., 2008. Quantitative Arsenic Speciation in Two Species of Earthworms from a Former Mine Site. *Journal Of Environmental Monitoring* **10**, 753-759.
- Webb, S. M., Gaillard, J. F., Ma, L. Q., and Tu, C., 2003. XAS Speciation of Arsenic in a Hyper-Accumulating Fern. *Environmental Science & Technology* **37**, 754-760.
- Wheatcroft, R. A., Jumars, P. A., Smith, C. R., and Nowell, A. R. M., 1990. A Mechanistic View of the Particulate Biodiffusion Coefficient: Step Lengths, Rest Periods and Transport Directions. *Journal of Marine Research* **48**, 177-207.
- Willoughby, G. L. and Kladivko, E. J., 2002. Water Infiltration Rates Following Reintroduction of *Lumbricus terrestris* into No-Till Fields. *Journal of Soil and Water Conservation* **57**, 82(7).
- Willoughby, G. L., Kladivko, E. J., and Reza Savabi, M., 1997. Seasonal Variations in Infiltration Rate Under No-Till and Conventional (Disk) Tillage Systems as Affected by *Lumbricus terrestris* Activity. *Soil Biology and Biochemistry* **29**, 481.
- Worm Watch, 2000. On-line Earthworm Taxonomic Key
<http://www.plantwatch.ca/english/wormwatch/resources/key/taxonomic.html>.
 EMAN Coordinating Office.
- Yeates, G. W., Orchard, V. A., Speir, T. W., Hunt, J. L., and Hermans, M. C. C., 1994. Impact of Pasture Contamination by Copper, Chromium, Arsenic Timber Preservative on Soil Biological Activity. *Biology and Fertility of Soils* **18**, 200-208.
- Zorn, M. I., Van Gestel, C. A. M., and Eijsackers, H., 2005a. The Effect of *Lumbricus rubellus* and *Lumbricus terrestris* on Zinc Distribution and Availability in

Artificial Soil Columns. *Biology and Fertility of Soils* **41**, 212.

Zorn, M. I., Van Gestel, C. A. M., and Eijsackers, H., 2005b. The Effect of Two Endogeic Earthworm Species on Zinc Distribution and Availability in Artificial Soil Columns. *Soil Biology and Biochemistry* **37**, 917.

Zorn, M. I., van Gestel, C. A. M., and Eijsackers, H. J. P., 2008. Metal Redistribution by Surface Casting of Four Earthworm Species in Sandy and Loamy Clay Soils. *Science of The Total Environment* **406**, 396.